

## INTRODUCTION

Confocal microscopy is a powerful tool for visualizing fluorescent specimens. The principal advantage of confocal microscopy over conventional wide-field microscopy is that it can reveal the three-dimensional structure of the specimen. Fluorescent specimens viewed with a conventional wide-field fluorescent microscope appear blurry and lack contrast because fluorophores throughout the entire depth of the specimen are illuminated, and fluorescence signals are collected not only from the plane of focus but also from areas above and below. A confocal microscope selectively collects light from a thin ( $<1\ \mu\text{m}$ ) optical section at the plane of focus in the specimen (Fig. 2C.1.1). Structures within the focal plane appear more sharply defined than with a conventional microscope because there is essentially no flare of light from out-of-focus areas. A three-dimensional view of the specimen can be reconstructed from a series of optical sections at different depths (Fig. 2C.1.2).

Several types of confocal microscopes are available. The most common type is the laser scanning confocal microscope (LSCM), which captures images by scanning the specimen with a focused beam of light from a laser and collecting the emitted fluorescence signals with a photodetector. LSCMs sometimes are referred to as “spot-scanning” confocal microscopes, to distinguish them from microscopes that scan the specimen with a slit of light (slit-scanning) or multiple spots of light (spinning-disk or Nipkow disk). Spot-scanning LSCMs have slower image acquisition rates than slit-scanning or spinning-disk microscopes ( $<1$  frame/sec versus 30 frames/sec or higher). However they are more versatile in a number of ways. They can accommodate lasers with a wide range of wavelengths (from the UV to the infrared) and can be configured to image multiple fluorophores either simultaneously or sequentially. Some include spectral detectors that can capture the entire spectrum of the fluorescence emitted at each pixel in the image. The most sophisticated LSCMs allow the user to control the illumination wavelength and intensity on a microsecond time scale. This feature makes it possible to perform experiments that require selectively illuminating fluorophores in a defined region of inter-

est in order to photobleach (Fig. 2C.1.1D) or photoactivate them. Measurement of fluorescence recovery after photobleach (FRAP) or fluorescence loss in photobleach (FLIP) can provide information about molecular mobility and binding (Cole et al., 1996; McNally and Smith, 2002; Lippincott-Schwartz et al., 2003; Sprague and McNally, 2005). Photosensitive molecules include certain fluorescent proteins (for example, see Patterson and Lippincott-Schwartz, 2002, for the fluorescent protein PaGFP and see Ando et al., 2002, for the photosensitive protein Kaede), “caged” molecules such as caged  $\text{Ca}^{2+}$  chelators, neurotransmitters, and second messengers (Nerbonne, 1996). Confocal microscopy also can be used to measure fluorescence resonance energy transfer (FRET; Wouters and Bastiaens, 2000).

In microbial research, confocal microscopy is widely used for applications that require visualizing microorganisms within their hosts (Roux et al., 2004; Fig. 2C.1.3A,B). Topics that have been addressed include the mechanisms of microbial adhesion and entry into host cells (Elphick et al., 2004; Ferrari et al., 2003), mechanisms of intracellular motility (Satpute-Krishnan et al., 2003; Viachou et al., 2004; Forest et al., 2005), and the reactions of host cells to infection (Perrin et al., 2004; Shaner et al., 2004). Confocal microscopy also has been used to characterize the growth and physical properties of biofilms (Drenkard and Ausubel, 2002; Rani et al., 2005; Daims et al., 2006; Fig. 2C.1.3C,D). The current generation of confocal microscopes, particularly those that utilize charge-coupled devices (CCDs) as photon detectors, are sufficiently sensitive to detect weak fluorescence signals and potentially could be used for imaging structures within individual microorganisms.

The purpose of this unit is to provide background information and practical tips for optimizing confocal imaging. The first section (Basis of Optical Sectioning) explains the basic principle of confocal imaging as implemented in a LSCM. The second section (Configuration of an LSCM) describes the components and light path in a typical LSCM and compares this with the light paths of spot-scanning microscopes and a new type of slit-scanning confocal microscope. The third

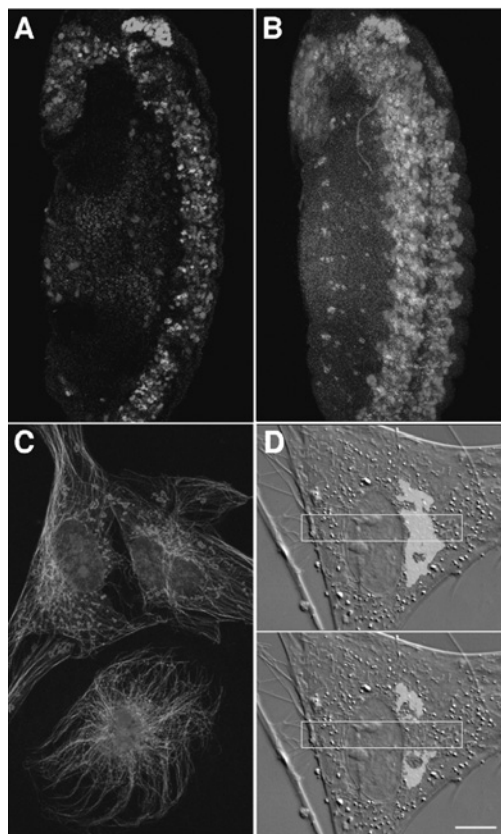


**Figure 2C.1.1** Applications of laser scanning microscopy. **(A, B)** Imaging in thick specimens. Neurons in a *Drosophila* embryo were immunolabeled with antibodies against three different transcription factors (images provided by Dr. Ward Odenwald of the National Institutes of Health, Bethesda, Md.; reproduced from Kamabadur et al., 1998). **(A)** A single optical section ( $\sim 2.5\text{-}\mu\text{m}$ ) captured with  $25\times$ , 0.8-NA objective. Labeled neurons in the plane of focus appear sharply defined, while those outside it are not visualized. **(B)** A maximum projection of 65 optical sections collected at  $2\text{-}\mu\text{m}$  intervals in the z axis. **(C)** Imaging intracellular structures. Dissociated rat fibroblasts were immunolabeled with anti-tubulin antibodies to visualize microtubules (green) and stained with fluorescent probes for mitochondria (Mitotracker, red) and DNA (DAPI, blue). The image is a projection of 20 optical sections ( $0.3\text{-}\mu\text{m}$  intervals) captured with a  $100\times$ , 1.4-NA objective. **(D)** Measuring molecular mobility in living cells. In a living fibroblast expressing a Golgi membrane protein (galactosyltransferase) fused to GFP (S65T), GFP fluorescence (green) is localized in the Golgi complex, shown superimposed on a DIC image of the cell. After the first image was collected, the boxed region (yellow) was scanned with full laser power to photobleach the GFP in the boxed area. The second image was collected 2 sec later. Subsequent images (not illustrated) showed that the GFP-galactosyltransferase rapidly diffused back into the photobleached area. Images were captured with a LSM410 (Carl Zeiss, Inc.). For the color version of this figure go to <http://www.currentprotocols.com>.

section (Practical Guidelines) provides guidelines for preparing specimens and configuring the critical parameters for confocal imaging. The Commentary provides references to sources of additional information.

### BASIS OF OPTICAL SECTIONING

Confocal microscopes accomplish optical sectioning by scanning the specimen with a focused beam of light and collecting the fluorescence signals emitted by the specimen

via a pinhole aperture. The pinhole aperture blocks signals from out-of-focus areas of the specimen whereas light from the focal plane passes through the pinhole to reach the detector. The physical basis of optical sectioning is illustrated in Figure 2C.1.4. The microscope objective focuses light from a point source (a laser) to a diffraction-limited spot in the specimen. The irradiation is most intense at the focal spot, but areas of the specimen above and below the focal spot are also illuminated. Fluorescent molecules excited by the incident light

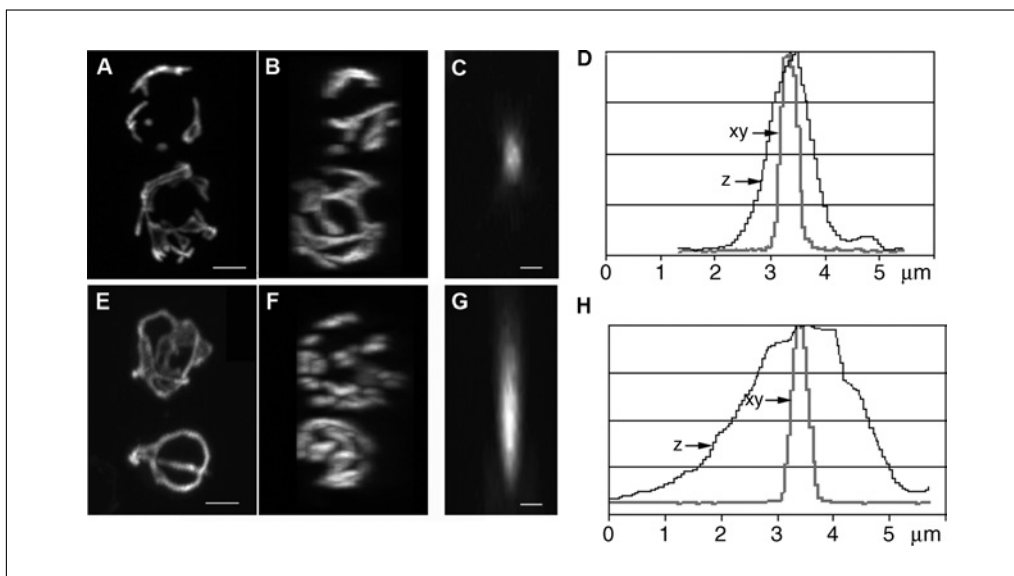


**Figure 2C.1.2** 3-D Imaging in living specimens. Comparison of water- and oil-immersion objectives. (A,B,E,F) Living yeast cells expressing a GFP construct that targets to the mitochondrial matrix were visualized with C-APO 63× 1.2 NA (water) objective (A,B) or a Planapochromat 100 × 1.4 NA (oil) objective (E,F). The images show xy and yz projections of stacks of 40 images collected at 0.2-μm intervals along the optical axis. The xy projections appear sharper than the yz projections because the resolution is higher in the focal plane of the objective than along the optical axis. The yeast were embedded in an aqueous solution with 0.2% agarose. Panels C and G are yz projections of images of 0.19-μm fluorescent beads captured with a 63× (water; C) or 100× (oil; G) objective. The beads were embedded in an aqueous solution with 2% agarose. D and H are intensity profiles along the horizontal and vertical axes of the beads. A 63× 1.2 NA (water) objective provides better axial resolution than an 100× 1.4 NA objective (oil) in specimens in an aqueous solution. Scale bars = 5 μm (A,B,E,F); 0.5 μm (C,G). Images were captured with a LSM510 (Carl Zeiss, Inc.).

emit fluorescence in all directions. The objective captures a portion of the emitted light. The objective projects light from the focal spot in the specimen to a conjugate spot in an “image” plane. The pinhole aperture is positioned in the image plane so as to be centered on this spot. The light that passes through the aperture is detected by a photomultiplier tube (PMT). Light from out-of-focus areas of the specimen is spread out at the image plane and is largely blocked by the pinhole aperture.

The diameter of the pinhole determines how much of the fluorescence emitted by the illuminated cone in the specimen is detected, as well as the thickness of the optical section. From wave optics, it is known that a point light source in the plane of focus of an objective produces a three-dimensional diffraction pattern in the image plane. The cross-section at the image plane is an Airy disk, a circular diffraction pattern with a bright central region. The radius of the bright central region of the Airy disk in the reference frame of the specimen is given by  $R_{\text{Airy}} = 0.61\lambda/\text{NA}$  where  $\lambda$  is the emission wavelength and NA is the numerical aperture of the objective (Inoué and Spring, 2002). At

the image plane, the radius of the central region is  $R_{\text{Airy}}$  multiplied by the magnification at that plane (Wilson, 1995).

Adjustment of the pinhole to a diameter slightly less than the diameter of the central region of the Airy disk allows most of the light from the focal point to reach the detector and reduces the background from out-of-focus areas by ~1000-fold relative to wide-field microscopy (Sandison et al., 1995). The separation of the in-focus signal from the out-of-focus background achieved by a properly adjusted pinhole is the principal advantage of confocal microscopy for examination of thick specimens.

Point illumination and the presence of a pinhole in the detection light path also produce improved lateral and axial resolution relative to conventional microscopy (Table 2C.1.1). The actual extent of improvement depends on the size of the pinhole. Near-maximal axial resolution is obtained with a pinhole radius of  $\sim 0.7 \times R_{\text{Airy}}$ , whereas optimal lateral resolution is obtained with a pinhole smaller than  $0.3 \times R_{\text{Airy}}$  (Wilson, 1995). However, a pinhole smaller than  $\sim 0.7 \times R_{\text{Airy}}$  significantly

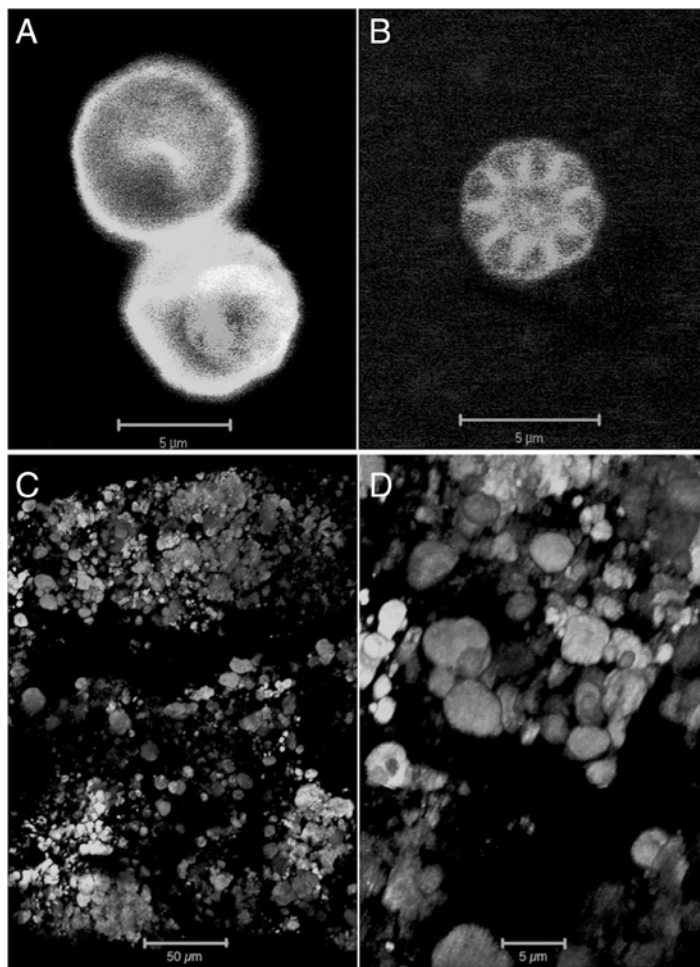


**Figure 2C.1.3** Applications of confocal microscopy in microbial research. (**A, B**). Human red blood cells (RBC) infected with malaria parasites (*Plasmodium falciparum*; 3D7 strain). Biotinylated human RBC were labeled with streptavidin-conjugated Quantum Dots 525 (CA; green color; <http://www.qdots.com>) and 0.5- to 4- $\mu$ M FM-64 (Molecular Probes, red color). The cells were injected into chambers (HybriWell HBW20 from Grace Bio-Labs) and were examined with an LSM 510 confocal microscope (Carl Zeiss, Inc.) with a 100 $\times$  1.4-NA oil objective. Panel A shows two RBC, one containing a parasite at the trophozoite stage; panel B shows a parasite at the schizont stage. The schizont was extruded from the RBC for better imaging of individual parasites (red). The green signal in the center of the schizont represents autofluorescence from hemazoin in the digestive vacuole. Images were provided by Dr. Svetlana Glushakova (National Institutes of Health, Bethesda, Md.; methods described in Glushakova et al., 2005). (**C, D**) Biofilm composed of microcolonies of nitrifying bacteria (ammonia oxidizers; *Nitrosomonas sp.*) and nitrite oxidizers (*Nitrospira sp.*). Both populations were labeled by fluorescence in situ hybridization (FISH) with 16S rRNA-targeted oligonucleotide probes. *Nitrosomonas* colonies are green; *Nitrospira* colonies are red. Images are 3-D reconstructions created using the *Daime* imaging program (see Daims et al., 2006, and Internet Resources) from stacks of optical sections collected with an LSM 510 (Carl Zeiss, Inc). Panel C shows an overview of the projected image of the biofilm, while panel D shows a smaller region at higher zoom. Images were provided by Dr. Holger Daims (Universität Wien, Vienna, Austria). For the color version of this figure go to <http://www.currentprotocols.com>.

reduces the total signal, a sacrifice that may not be worth the gain in resolution, especially when imaging dim samples. In fluorescence

imaging, resolution is also influenced by the emission and excitation wavelengths (Table 2C.1.1).

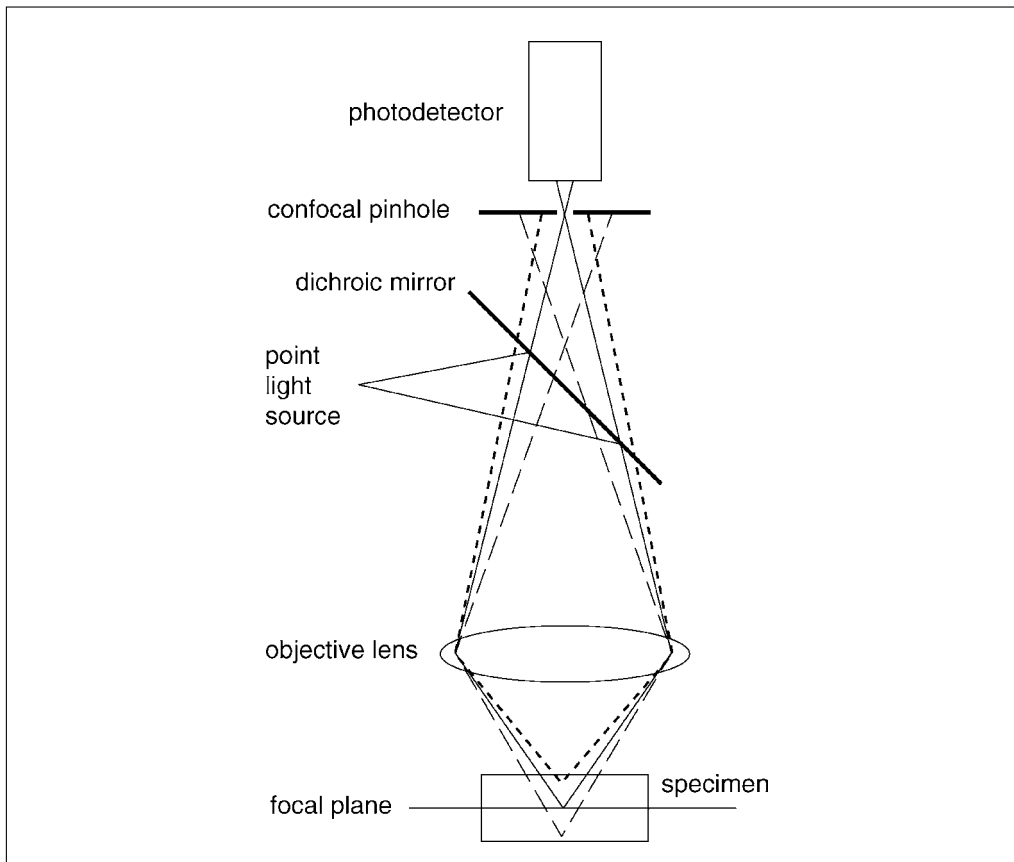


**Figure 2C.1.4** The basis of optical sectioning. Illumination from a point light source is reflected by a dichroic mirror into the back aperture of a microscope objective. The objective lens focuses the light to a diffraction-limited spot within the specimen. Fluorophores at the focal spot and within the cones of illumination above and below it are excited, emitting fluorescence in all directions. The fluorescence captured by the objective passes through the dichroic mirror because the fluorescence is at a longer wavelength than the excitation. The confocal pinhole allows fluorescence from the focal spot to reach the photodetector and blocks fluorescence from out-of-focus areas. Redrawn from Shotton (1993).

**Table 2C.1.1** Theoretical Resolutions of Confocal and Conventional Microscopes<sup>a,b</sup>

$\lambda_x/\lambda_{em}$	Objective					
	10×, 0.4 NA, air		40×, 0.85 NA, air		60×, 1.4 NA, oil	
	Lat. res.	Ax. res.	Lat. res.	Ax. res.	Lat. res.	Ax. res.
<i>Confocal fluorescence microscope</i>						
488/518	0.55	4.50	0.26	0.99	0.16	0.56
568/590	0.64	5.17	0.30	1.09	0.18	0.64
647/677	0.72	5.88	0.34	1.28	0.21	0.72
<i>Conventional fluorescence microscope</i>						
518	0.79	6.48	0.37	1.43	0.24	0.93
590	0.90	7.38	0.42	1.63	0.28	1.06
680	1.04	8.50	0.49	1.88	0.32	1.22

<sup>a</sup>Data reprinted from Brelje et al. (1993) by permission of Academic Press.

<sup>b</sup> $\lambda_{ex}$  and  $\lambda_{em}$ , excitation and emission wavelengths; lat. res. and ax. res., lateral and axial resolutions.

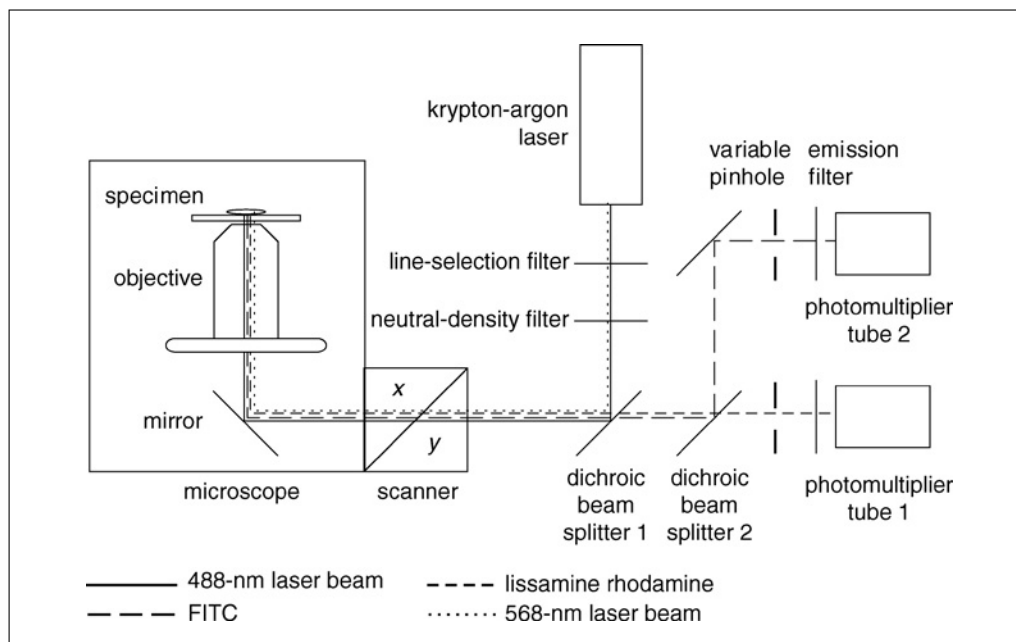


**Figure 2C.1.5** The light path of a laser-scanning confocal microscope. The diagram illustrates the light path of a LSCM set up for simultaneous imaging of FITC and lissamine rhodamine. The 488- and 568-nm lines of a krypton-argon laser are reflected by dichroic beam splitter 1 into the optical axis of the microscope. The beam is reflected by a mirror into the microscope objective, which focuses the beam to a diffraction-limited spot in the specimen. The scanner consists of a pair of galvanometer mirrors that deflect the laser beams so as to scan the spot across the specimen in a raster pattern. Fluorescence emitted as each point is illuminated travels the reverse path through the scanning system. The FITC fluorescence (peak at 520 nm) and lissamine rhodamine fluorescence (peak at 590 nm) pass through dichroic beam splitter 1 to dichroic beam splitter 2, which transmits the lissamine rhodamine fluorescence to photomultiplier tube 1 and reflects the FITC fluorescence to photomultiplier tube 2. A variable pinhole in front of each photodetector blocks light from out-of-focus areas of the specimen while allowing light from the focal plane to reach the detector.

### CONFIGURATION OF AN LSCM

Confocal microscopes use lasers for illumination because they provide intense excitation within a narrow range of wavelengths. Mixed krypton-argon gas lasers are popular for multicolor confocal microscopy because they emit at three wavelengths (488, 568, and 647 nm) that excite many commonly-used fluorophores—e.g., FITC, rhodamine, Cy3, Cy5, Alexa 488/555/568/647, green fluorescent protein (GFP), and red fluorescent protein (mRFP or DsRed). The disadvantage of krypton-argon lasers is that their life spans are short (~2000 hr). Another way to achieve multiwavelength excitation is to combine the outputs of multiple lasers. Many of the confocal microscopes currently on the market combine an argon laser (488 nm) with a green helium-neon (HeNe) laser (543 or 594 nm) and a red HeNe laser (633 nm). The argon laser also may provide 458 and 514 nm lines, which can be used to excite the cyan and yellow variants of GFP (CFP and YFP). Some confocal microscopes can accommodate a 405-nm diode

laser. The 405-nm laser is more optimal for excitation of CFP than the 458 line of the argon laser and also excites photosensitive GFP (PaGFP). It can even be used to visualize some UV fluorophores such as DAPI and Hoechst DNA dyes, although 405 nm is not the optimal excitation wavelength for these dyes. UV argon lasers (351/364 nm) also are available. Inclusion of a 405 nm or UV argon laser adds considerably to the cost of the confocal microscope system due to the requirement for additional optical components to handle these wavelengths.

The light path in a simple confocal microscope is illustrated in Figure 2C.1.5. The output of the laser (or the combined output of multiple lasers) is reflected into the optical axis of the microscope by the primary dichroic beam splitter (splitter 1 in Fig. 2C.1.5). Wavelength-selection filters are inserted into the light path to block specific laser lines, and neutral-density filters may be inserted to attenuate the illumination. In current, high-end confocal

systems, the line selection and neutral-density filters have been replaced with an electronically controlled acousto-optical tunable filter (AOTF). An AOTF can alter its transmission characteristics so as to pass selected wavelengths, while completely blocking others. An AOTF also provides precise control over the attenuation of the individual laser beams.

The scanner deflects the laser beam into the objective at varying angles in order to scan the laser beam across the specimen. Several different technologies for scanning have been devised. The most common method employs a pair of galvanometer mirrors. One mirror oscillates rapidly to excite sequential spots along the *x*-axis of the specimen, and the second mirror oscillates more slowly to move the illumination from line to line in the *y*-axis.

The fluorescence emissions that are collected by the objective follow the reverse path through the scanner to the primary dichroic beam splitter, and thereby are “descanned” (Fig. 2C.1.5). The fluorescence signals (which are at a longer wavelength than the excitation due to the Stokes shift; are transmitted through the beam splitter. To simultaneously image fluorescence from multiple fluorophores requires selection of a primary dichroic beam splitter that reflects each of the required excitation wavelengths and transmits the emissions of all of the fluorophores. Secondary dichroic mirrors split the fluorescence emissions from different fluorophores for detection by separate detectors. Emission filters are inserted in the light path to the detectors (Fig. 2C.1.5) to block back-scattered excitation light and to reduce bleed-through of signals between channels. Current high-end confocal microscopes use more sophisticated technology for emission discrimination; descriptions of the designs of specific systems are available from the vendors (see *SUPPLIERS APPENDIX*).

The fluorescence captured by the objective focuses to a stationary spot (Airy disk) in the image plane (Fig. 2C.1.4). The pinhole aperture is positioned in the image plane so as to be centered on the Airy disk. The diameter of the pinhole aperture can be adjusted to allow optimization for different Airy-disk sizes, which vary with the objective’s numerical aperture and the emission wavelength. Adjustment of the diameter of the pinhole to a value of 0.7 to 1.0 Airy Unit allows most of the in focus light to reach the detector and blocks most of the out-of-focus light. In systems with a separate pinhole aperture for each detector, the pinhole apertures are located immediately in

front of the detectors. Incorporation of a separate pinhole for each detector allows the user to optimize the pinhole settings for different wavelengths.

The photodetectors in LSCMs are photomultiplier tubes (PMTs), which generate electrons at a rate proportional to the intensity of the incoming fluorescence signal (Art, 1995). The PMT output is converted to a digital image that can be displayed on a computer monitor and stored as a digital file for later analysis. Digitization may be at 8-bit (256 gray levels), 10-bit (1024 gray levels) or 12-bit resolution (4096 gray levels). Confocal microscopes typically have two to four PMTs for reflected light/epifluorescence imaging and may have, in addition, a photodetector for transmitted light.

In spinning disk confocal microscopes, the illumination from a laser or white light source passes through pinholes in the Nipkow disk so as to excite fluorescence at multiple (~1000) sites within the specimen. The disk revolves rapidly (1000 to 5000 rpm) causing the illuminating spots to sweep across the specimen as uniformly-spaced scan lines (Inoué and Inoué, 2002). Fluorescence emitted by the specimen that is collected by the objective returns through the same pinholes in the Nipkow disk that provided the excitation light before it is detected by a full-field CCD camera. In this way, point light sources and detector pinholes to block out-of-focus fluorescence are provided, with the advantage of higher collection speeds than a spot scanner. Drawbacks of this approach include decreased illumination to the specimen from light loss through the pinholes and the inability to change the pinhole diameter. This means that, unlike the case with a spot scanner, optimal confocality is achieved only for one objective magnification, and the thickness of the optical section cannot be changed. Although the reduced specimen illumination generates a smaller fluorescent signal, scientific-grade CCD cameras have significantly higher quantum efficiencies than the PMTs used for fluorescence detection in LSCMs and are able to more than adequately detect these levels of fluorescence. Fluorescent specimens have been reported to undergo less photobleaching during examination with a spinning disk confocal microscope than with a LSCM. The lower rate of photobleaching is thought to be due to the lower illumination levels (Inoué and Inoué, 2002).

A new type of slit-scanning confocal microscope (LSM 5 Live; Carl Zeiss, Inc.) that allows images to be acquired at rates as fast

as or faster than can be achieved with a spinning disk confocal microscope and with as low or lower rates of photobleaching has recently been introduced. The system adopts principles from both the spot scanner and the spinning disk in that it uses a single scanning galvanometer to move an illumination line that is combined with a sensitive single-line CCD detector. The point source of light from the laser is optically converted to a narrow line, which is reflected onto the specimen by a novel beam splitter consisting of a mirrored line on transparent glass. The line illumination is scanned across the specimen. The emitted fluorescence from the specimen that is collected by the objective passes through the beam splitter and is detected by a linear CCD detector. A slit aperture in front of the detector blocks out-of-focus light, analogous to the pinhole aperture in an LSCM. The LSM 5 Live has somewhat poorer resolution than a spot-scanning LSCM, and the initial version is less versatile but can capture images much more rapidly.

## PRACTICAL GUIDELINES

### Sample Preparation

The preeminent goal in preparing samples for imaging with a confocal microscope is to maximize the fluorescence signals while preserving the three-dimensional structure of the specimen. Ideally, the sample should be less than  $\sim 50 \mu\text{m}$  in thickness, although thicker samples can be visualized. Guidelines for preparing fixed and living samples are described below.

### Fixation

A standard fixative for fluorescence microscopy is 2% to 4% formaldehyde in PBS. Formaldehyde penetrates cells rapidly and preserves the antigen-recognition sites for many antibodies. However, formaldehyde cross-links proteins slowly and may cause vesiculation of membranes. Some commercial preparations of formaldehyde (formalin) contain methanol, which shrinks cells. Techniques for optimizing formaldehyde fixation are described by Bacallao et al. (1995). Fixatives containing a small amount of glutaraldehyde (0.125% to 0.25%) in addition to formaldehyde preserve cellular morphology better, but glutaraldehyde destroys the epitopes for some antibodies. Glutaraldehyde fixation induces

autofluorescence but autofluorescence can be reduced by treating the sample after fixation with  $\text{NaBH}_4$  (1 mg/ml in PBS, pH 8.0, using two treatments of 5 min each for dissociated cells, longer for thicker samples). An alternative procedure for preparing specimens for immunocytochemistry is to immerse them in cold ( $-20^\circ\text{C}$ ) methanol or acetone but fixation by this method causes severe shrinkage.

### Choices of fluorophores

The choice of fluorophores should take into account the available laser lines and the detector channels of the confocal microscope. Excitation is most efficient at wavelengths near the peak of the excitation spectrum of the fluorophore, but a precise match is not required. For experiments that require imaging multiple fluorophores with standard photodetectors (PMTs), it is best to select fluorophores that are excited by different laser lines, in order to minimize spectral crossover (bleed-through) between the channels (Fig. 2C.1.6). Excitation and emission spectra for many fluorophores are available via the Internet (see Internet Resources). A recommended combination of fluorophores for excitation at 405 nm, 488 nm, 543/561 nm, and 633 nm would comprise Marina Blue, Alexa 488, Alexa 555, and Alexa 647 (all available from Molecular Probes/Invitrogen). The nucleic acid stain DAPI can be excited by illumination at 405 nm, although ultraviolet excitation (350 nm) is more optimal. The cyanine dyes Cy2, Cy3, and Cy5 (available from Jackson ImmunoResearch Laboratories) are also suitable for confocal microscopy. For multiwavelength imaging with a spectral detector and spectral unmixing, it is important to select fluorophores that have distinct emission spectra, but there is no advantage in using fluorophores that have differing excitation spectra. Indeed, it is best to use fluorophores that have similar excitation maxima, so that they can be excited with a single laser line reflected into the microscope with a single-wavelength dichroic mirror. Other important criteria to consider in selecting fluorophores for confocal microscopy are the quantum efficiencies and rates of photobleaching. In addition, the staining protocol should be designed so as to produce similar signal intensities in each channel. More information about selecting fluorophores for confocal imaging is available at the Molecular Expressions Web site (see Internet Resources).

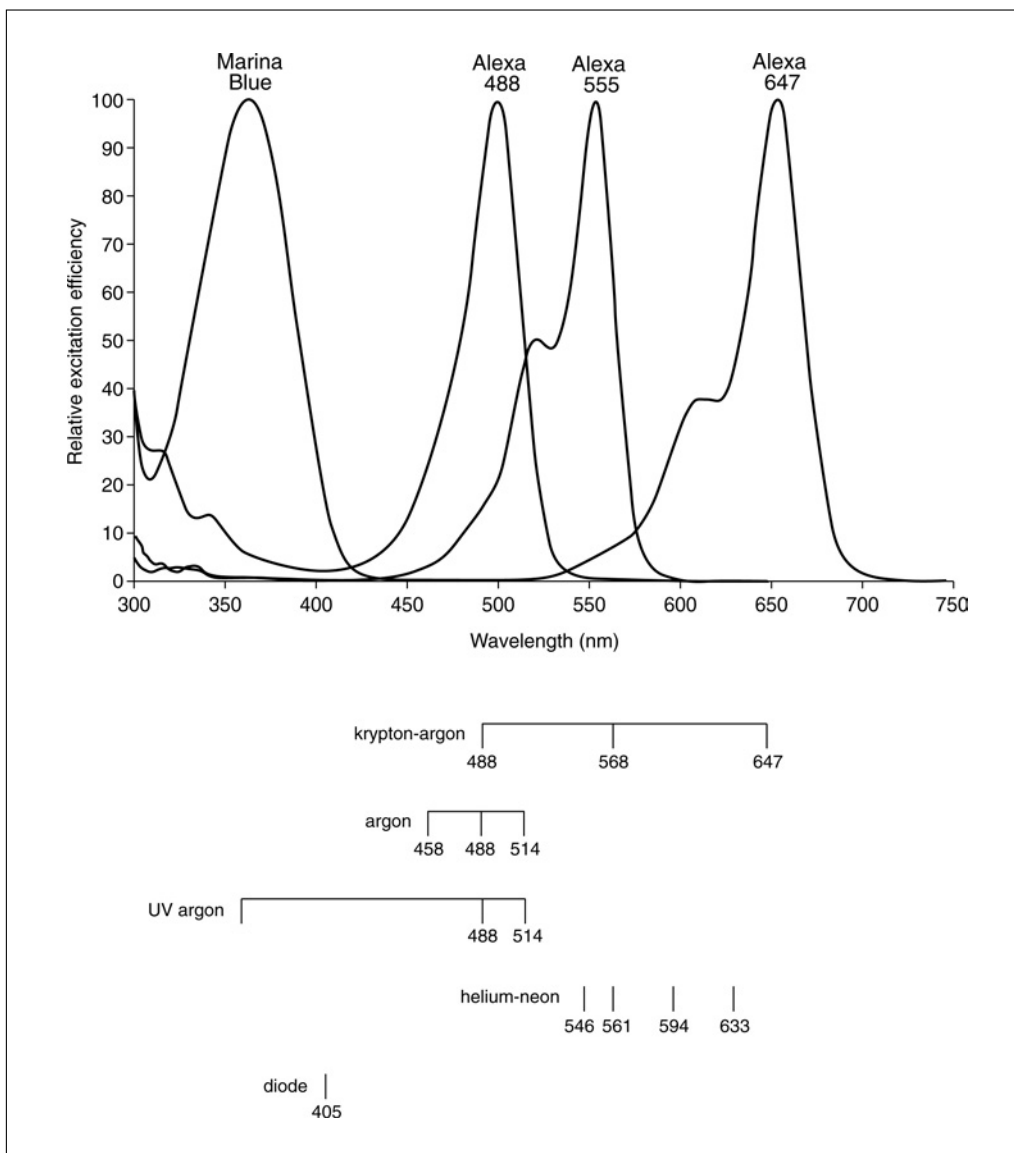


**Figure 2C.1.6** Excitation spectra of representative fluorophores and emission wavelengths of lasers for confocal microscopy. The graph at the top shows the excitation spectra of Marina Blue, Alexa 488, Alexa 555, and Alexa 647 (Molecular Probes). The emission wavelengths of lasers commonly used for confocal microscopy are shown below. Data for the excitation spectra are from Molecular Probes.

### **Control samples**

Confocal microscopes rely on electronic image enhancement techniques that can make even dim autofluorescence signals or non-specific background staining look bright. In order to distinguish a real signal from background, it is essential to prepare and examine appropriate control samples. For immunofluorescence experiments with one primary antibody, the appropriate control samples are unstained specimens and specimens treated with the secondary antibody but no primary antibody. Other control experiments may be required to verify the specificity of labeling. Experiments with two primary and secondary

antibodies require additional controls to test whether the secondary antibodies cross-react with the “wrong” primary antibody. Singly stained samples also should be prepared and imaged to determine the extent of spectral cross-over between the channels.

### **Mounting the specimen**

Selection of a mounting medium should take into account the type of microscope objective that will be used to observe the specimen (see section on Microscope Objectives). In order for an objective to perform optimally, the mounting medium should have the same refractive index as the objective immersion

**Table 2C.1.2** Refractive Indexes of Common Immersion and Mounting Media

Medium	RI
<i>Immersion media</i>	
Air	1.00
Water	1.338
Glycerol	1.47
Immersion oil	1.518
<i>Mounting media</i>	
50% glycerol/PBS/DABCO	1.416 <sup>a</sup>
5% <i>n</i> -propyl gallate/0.0025% <i>p</i> -phenylene diamine (PPD) in glycerol	1.474 <sup>a</sup>
0.25% PPD/0.0025% DABCO/5% <i>n</i> -propyl gallate in glycerol	1.473 <sup>a</sup>
VectaShield (Vector Labs)	1.458 <sup>a</sup>
Slow Fade (Molecular Probes)	1.415 <sup>b</sup>
ProLong (Molecular Probes)	1.3865 <sup>b,c</sup>

<sup>a</sup>Data from Bacallao et al. (1995).

<sup>b</sup>Data from Molecular Probes.

<sup>c</sup>Refractive index (RI) for liquid medium. (RI for solidified medium will be higher.)

medium. Mismatches in the refractive indices produce spherical aberration leading to loss of light at the detector, as well as decreased *z*-axis resolution and incorrect depth discrimination. Image deterioration caused by spherical aberration increases with depth into the specimen; therefore, matching the immersion and mounting medium refractive indices is particularly important for thick specimens. The refractive indices of some commonly used mounting media are listed in Table 2C.1.2.

Mounting media that have refractive indices close to that of immersion oil (RI = 1.51) include DPX (RI = 1.5; ProSciTech) and Permount (RI = 1.52; ProSciTech). However, specimens must be dehydrated prior to mounting in these media, and dehydration causes shrinkage and distortion. Moreover, some fluorophores cannot withstand dehydration. Cells retain their three dimensional shapes when they are kept in physiological saline (PBS) or a mixture of PBS and glycerol (Bacallao et al., 1995). If the specimen is to be mounted under a coverglass, it may be necessary to support the coverglass to avoid damaging the specimen.

Addition of an antioxidant (antifade agent) to the mounting medium helps to alleviate photobleaching of synthetic fluorophores such as those used for immunocytochemistry. One of the best antifade agents is 100 mg/ml 1,4-diazabicyclo[2,2,2]octane (DABCO; Sigma; Bacallao et al., 1995). *n*-propyl gallate (Giloh and Sedat, 1982) and *p*-

phenylenediamine (PPD; Johnson et al., 1982) are also effective antifade agents, but the former may cause dimming of the fluorescence while the latter may damage the specimen (Bacallao et al., 1995). A wide variety of mounting media are available from commercial sources (Biomedica, Electron Microscopy Sciences, ProSciTech, Molecular Probes, Vector Laboratories) and many of these contain antifade agents. It is wise to check with the fluorophore provider for recommendations about which mounting medium and antifade agents to use. Antioxidants do not reduce photobleaching of fluorescent proteins.

### *Living specimens*

Microscopy on living specimens grown *in vitro* is most conveniently performed with an inverted microscope, because the specimens can be viewed through the bottom of the culture chamber and the top can be opened for access. To allow imaging with an oil- or water-immersion objective, the culture chamber substrate should be a coverglass. The glass coverslip can be coated with poly-L-lysine (using a 1 mg/ml solution; Sigma) to promote adhesion of the specimens (either eukaryotic cells or microorganisms). Nonadherent specimens can be immobilized by embedding them in a thin layer of low-melting-point agar (0.2% for eukaryotic cells, up to 2% for smaller organisms). Motile specimens

such as *Paramecium* can be attached to the substrate with CellTak (BD Biosciences; W. Bell, pers. comm.). Culture chambers with coverglass substrates can be made from standard plastic petri dishes by boring holes in their bottoms and affixing coverglasses to the holes with Silgard (Dow-Corning). Culture chambers with coverglass substrates are also available from commercial sources (Labtek coverglass chamber, Fisher Scientific; MatTek glass-bottom culture dish, MakTek Corp). Alternatively, cells may be grown on a coverglass that can be mounted in a chamber for observation on a microscope. A simple chamber can be constructed from a gasket cut from a sheet of silicon rubber or a soft plastic ruler and affixed to a glass microscope slide with silicon grease. The well formed by the gasket is filled with medium, and then the coverglass with cells attached is sealed onto the well. More elaborate chambers, some having built-in heaters and/or ports for perfusion, are available from commercial sources (see Internet Resources for a list of suppliers).

Specimens that need to be kept warm during observation pose a particular challenge because temperature transients can make it difficult to maintain focus. Probably the best way to keep specimens warm is to place the entire microscope in a temperature-controlled enclosure. Alternative strategies include warming the microscope stage with heated air (using an air stream incubator or hair dryer) or infrared lamps, or using a temperature-controlled specimen chamber (Terasaki and Dailey, 1995). If an oil or water immersion objective is used, heating the objective helps to maintain the specimen at the desired temperature. Microscope enclosures, stage warmers, temperature-controlled chambers, and objective heaters are available from suppliers of microscopes and microscope accessories.

Living specimens should be kept in a medium that is buffered to maintain the correct pH. Many commonly used culture media are buffered with bicarbonate and require an atmosphere with 5% to 10% CO<sub>2</sub> to maintain the correct pH. For microscopy, it is more convenient to use a buffer that maintains the correct pH in air. Many types of cells can be maintained for several hours in a balanced saline solution or culture medium that is buffered with HEPES (10 to 20 mM). Use of a medium that contains phenol red should be avoided because phenol red adds background fluorescence and can produce oxygen radicals when exposed to intense illumination. Addition of 0.3 U/ml Oxyrase (Oxyrase, Inc.) to the medium can

help to alleviate photobleaching of synthetic fluorophores (Waterman-Storer et al., 1993).

## Optimizing Imaging Parameters

### *Microscope objectives*

High-NA objectives are optimal for fluorescence microscopy because they collect more light than low-NA objectives (brightness is proportional to NA<sup>4</sup>). Oil-immersion objectives have the highest numerical apertures (NA = 1.4 or 1.45). However, oil-immersion objectives have short working distances (100 to 200 μm). Moreover, they work optimally only with specimens mounted in a medium with a refractive index the same as that of immersion oil ( $n = 1.51$ ). Mismatch of the refractive indices leads to a deterioration of image quality that becomes increasingly severe with depth into the specimen. When a high-NA oil objective is used to image a specimen mounted in an aqueous medium, image quality and signal brightness decline noticeably at distances of 5 to 10 μm from the coverglass. Mismatch of the refractive indices also leads to spatial distortion in the  $z$ -axis. The actual movement of the focal plane in the specimen ( $d_s$ ) produced by a movement of the objective ( $d_{obj}$ ) depends on the ratio of the refractive indexes:  $d_s/d_{obj} = \eta_s/\eta_{obj}$  (Majlof and Forsgren, 2002).

A water-immersion objective is useful for imaging living specimens that are more than a few microns thick. Water-immersion objectives with numerical apertures of 1.2 are available. These objectives are designed for viewing specimens mounted under a coverglass (0.17 μm; no. 1.5) and have fairly short working distances (130 to 220 μm). “Dipping” objectives, which are intended for use without a coverglass, have lower numerical apertures (NA = 0.9) and longer working distances (1 to 2 mm).

Objectives differ in their transmission efficiency and degree of correction for spherical and chromatic aberration and flatness of field. Plan Apochromat objectives provide the flattest fields of view and color correction for three wavelengths. Plan Apochromat objectives generally transmit efficiently throughout the visible spectrum (400 nm to 700 nm), but may transmit poorly in the UV (<400 nm) or infrared (>700 nm; Keller, 1995). Some objectives that are less highly corrected (Fluar, Plan NeoFluar, Plan Fluor) provide higher transmission at visible, UV, and infrared wavelengths. For additional information about objectives for confocal microscopy see

the *UNIT 2A.1*, Keller (1995), Benham (2002), and the Molecular Expressions Web site (see Internet Resources).

### ***Pinhole size***

As explained in the section on the Basis of Optical Sectioning, the size of the detector pinhole has a critical influence on image quality. A pinhole with a diameter slightly less than or equal to the diameter of the bright central region of the Airy disk will let most of the light from the plane of focus reach the detector, while blocking most of the out-of-focus flare. The lateral resolution will be  $\sim 10\%$  better than that obtainable by conventional microscopy with the same optics (Centonze and Pawley, 1995), although not as good as can be achieved with a smaller pinhole. Lateral resolution continues to improve as pinhole radius is decreased down to a pinhole size of  $\sim 0.2 \times$  Airy disk radius, but a pinhole this small excludes  $\sim 95\%$  of the signal (Wilson, 1995). Axial resolution improves as pinhole size decreases, down to  $\sim 0.7 \times$  Airy disk radius, then levels off. The best trade-off between signal intensity and resolution will depend on the characteristics of the sample and the required resolution.

### ***Scan zoom***

The scan zoom determines the dimensions of the area in the specimen that is scanned. Increasing the zoom reduces the dimensions of the scan area. The pixel number remains the same; consequently, individual pixels represent a smaller area. For example, the scan area at zoom 2 is one quarter the scan area at zoom 1 and the pixel dimensions are half as large in each dimension. That is, if the pixel dimensions represent  $0.25 \mu\text{m} \times 0.25 \mu\text{m}$  at zoom 1, then dimensions are  $0.125 \times 0.125 \mu\text{m}$  at zoom 2.

For each objective, there is an optimal zoom setting that yields pixel dimensions sufficiently small to take advantage of the full resolution of the objective but large enough to avoid oversampling. In order for the minimum resolvable entity to be visible on the display monitor, the pixel dimension needs to be smaller than (less than one-half) the optical resolution. However, if the pixel size is made too small by using a higher-than-optimal zoom factor, the specimen is subjected to more irradiation than necessary, with an increased risk of photobleaching. The rate of photobleaching increases proportionally to the square of the zoom factor (Centonze and Pawley, 1995). A guideline for selecting an appropriate zoom

factor derived from information theory (the Nyquist Sampling Theorem) states that the pixel dimensions should be equal to the optical resolution divided by 2.3 (see Webb and Dorey, 1995). The optical resolution in confocal imaging depends on the numerical aperture of the objective, the refractive index of the immersion medium, the excitation and emission wavelengths, and the diameter of the pinhole aperture. Values calculated for different objectives and wavelengths using the point-spread functions (PSF) for wide-field and confocal microscopy are given in Table 2C.1.1. The lateral resolution for confocal microscopy can be approximated by:  $\text{Resel}_{x,y \text{ confocal}} = 0.4\lambda/\text{NA}$ , where  $\lambda$  is the wavelength of the illumination and NA the numerical aperture of the objective (see Webb and Dorey, 1995). The above equation assumes the use of an infinitesimal pinhole;  $\text{Resel}_{x,y}$  will be larger with a pinhole of 0.7 to 1 Airy unit.

### ***z-axis sectioning interval***

In order to study the three-dimensional structure of a specimen, a series of images are captured at fixed intervals throughout the entire depth of the specimen. The interval between focal planes needed to achieve optimal resolution in the  $z$ -axis is not as small as the  $x,y$  pixel dimensions because the axial resolution is poorer than the lateral resolution (see Table 2C.1.1). The optimal interval (according to the Nyquist Sampling Theorem) is equal to the axial resolution divided by 2.3. The axial resolution for an objective in confocal imaging can be approximated by:  $\text{Resel}_z \text{ confocal} = 1.4\lambda n/\text{NA}^2$  where  $n$  is the refractive index (see Webb and Dorey, 1995). Collecting images at shorter intervals results in oversampling, with an increased risk of photobleaching.

### ***Illumination intensity***

Fluorescence emission increases linearly with illumination intensity up to a level at which emission saturates. Optimal signal-to-background and signal-to-noise ratios are obtained with illumination levels well below saturation (Tsien and Waggoner, 1995). The illumination intensity on a laser-scanning microscope can be adjusted by operating the laser at submaximal power and by inserting neutral-density filters into the light path or varying the transmission through the AOTF. In general, the best images are obtained with illumination levels that are as high as possible without producing unacceptable rates of photobleaching.

### ***PMT black level and gain***

The contrast and background of confocal images are determined by the gain and black-level settings of the photomultiplier tube (PMT) amplifiers. To obtain maximal information, the black level and gain should be adjusted to take advantage of the full dynamic range of the PMTs. The appropriate black-level setting can be found by scanning while the light path to the PMT is blocked. The image that appears on the display monitor should be just barely brighter than the background, which is black (gray level = 0). To set the gain, scan the specimen and adjust the gain so that the brightest pixel in the image is slightly below white (gray level = 255, for 8-bit images). Ensuring that all signals fall within the dynamic range of the PMT is especially important for quantitative imaging experiments. Confocal imaging software typically includes a pseudocolor image display mode (“range indicator”) that facilitates selection of appropriate black level and gain settings by highlighting pixels with intensity values near 0 or 255.

### ***Averaging***

Confocal images of dimly fluorescent specimens captured at the fastest scan rate on a typical LSCM (~0.5 sec/frame) appear noisy because of the small numbers of photons collected from each spot. Improved signal-to-noise can be attained by scanning the specimen at a slower rate or by scanning multiple times and averaging the signals. Current LSCMs allow individual lines in the image to be repeatedly scanned and averaged. Line averaging generally produces sharper images than frame averaging (which averages full frames) because there is less risk of blurring due to movements or changes in the specimen.

### ***Imaging multiple fluorophores***

Confocal microscopes can typically be configured to capture images of two or more fluorophores simultaneously or sequentially. Each approach has advantages and disadvantages. For simultaneous imaging, the specimen is scanned with all of the required excitation wavelengths and the emissions of the different fluorophores are split for detection by separate photodetectors (Fig. 2C.1.5). The drawback of this approach is that spectral cross-over between channels may occur if the emission spectra of the fluorophores overlap. If each fluorophore is excited by only one laser line, then exciting them sequentially will avoid spectral cross-over. The disadvantage of sequential excitation is that there may

be misalignment of the signals in different channels, particularly if the specimen is alive and moving. A third way of imaging multiple fluorophores is available in confocal systems in which the laser excitation is controlled with an AOTF; such systems can scan each line of the specimen sequentially with different excitation wavelengths with a time delay between scan lines of less than a millisecond. Line-by-line wavelength switching provides rapid acquisition of fluorescence signals from each spot in the specimen while avoiding the spectral cross-over between channels that may occur when the fluorophores are excited simultaneously.

### ***Image display***

Confocal images are typically displayed as 8-bit grayscale or 24-bit RGB (red/green/blue) color images. Each channel of an RGB image can represent a different fluorophore (Fig. 2C.1.1A to C). Color mixtures indicate colocalization of fluorophores within a pixel. A RGB fluorescence image can be merged with a grayscale transmitted light image by adding the transmitted light image to each channel of the RGB image (Fig. 2C.1.1D; fluorescence in green channel merged with DIC image).

The three-dimensional dataset obtained by capturing a series of optical sections through the specimen can be used to compute views of the specimen from different viewing angles. Commercial confocal microscopes typically include the capability to generate orthogonal views of the specimen ( $xy$ ,  $xz$ , and  $yz$ ) and may permit views from arbitrary angles. An  $xy$  projection or “z-series projection” is a two-dimensional display formed by merging multiple image planes (Fig. 2C.1.1B,C, Fig. 2C.1.2A,E). The most common type of projection is a “maximum” projection in which each pixel represents the intensity of the brightest pixel in the  $z$ -axis. Another type of projection, referred to as “surface render,” displays the most superficial pixels with intensities above a defined threshold. Projections also can be created for different viewing angles (Fig. 2C.1.2B, F). Projections of the specimen from different viewing angles can be combined to create an animation in which the specimen appears to rotate in space. Such animations give the viewer a striking impression of the three-dimensional geometry of the specimen. Generating two projections at azimuths differing by  $4^\circ$  to  $10^\circ$  creates stereo pairs that can be visualized with a stereo viewer or color-coded and merged to form a stereo anaglyph. Volume-rendering

imaging software is available that provides additional options for three-dimensional visualization and measurements (see Internet Resources).

## COMMENTARY

Effective use of a confocal microscope requires understanding of the principles of image formation and knowledge of how to set up and use a microscope. The unit on Proper Alignment and Adjustment of the Light Microscope (UNIT 2A.1) describes the components of a light microscope and provides protocols for setting up a microscope for transmitted light and epifluorescence imaging. This unit also lists references to literature on light microscopy. *The Handbook of Biological Confocal Microscopy* (edited by V. Centonze and J. Pawley, 1995, new edition planned for March 2006) is a comprehensive reference book on confocal microscopy. It includes chapters on the fundamental principles, instrumentation, image acquisition and display, sample preparation, and much more. *Confocal Microscopy* (Wilson, 1990) provides a thorough discussion of the principles behind confocal imaging. *Cell Biological Applications of Confocal Microscopy* (edited by B. Matsumoto, 2002) discusses the performance of different types of confocal microscopes and contains practical information about common applications such as imaging immunofluorescence and calcium ion indicators. Additional applications are described in *Confocal and Two Photon Microscopy: Foundations, Applications and Advances* (Diaspro, 2002). The Molecular Expressions Web site also is an excellent source of information about light microscopy, including confocal microscopy (see Internet Resources).

Confocal microscopy is only one of several available techniques for capturing optical sections in fluorescent specimens. An alternative to confocal microscopy is computational “deconvolution” of images captured by wide-field epifluorescence microscopy (McNally et al., 1999; Boccacci and Bertero, 2002). Computational deconvolution makes use of all of the fluorescence captured by the objective, in contrast to confocal microscopy, which discards fluorescence from out-of-focus areas. In addition, wide-field microscopy can employ CCD cameras that have higher quantum efficiencies than the photodetectors used for confocal microscopy. For these reasons, wide-field microscopy and deconvolution can be superior to confocal microscopy for imaging dim specimens or specimens that are susceptible to photobleaching or photodamage.

However, computational deconvolution of images is time-consuming and does not work well in specimens with high levels of dispersed fluorescence. Confocal microscopy allows direct visualization of optical sections and is applicable to a wider range of specimens.

Another technique for confocal imaging takes advantage of the optical phenomenon known as multiphoton excitation. Multiphoton microscopy allows deeper penetration into tissue than either wide-field microscopy or conventional (single-photon) microscopy, and is particularly useful for imaging in thick specimens such as tissue slices or multicellular organisms. However, this method suffers loss of resolution due to the longer illumination wavelength and absence of a detector pinhole.

## Troubleshooting

Test samples are useful for monitoring the performance of a confocal microscope. A micrometer slide should be used to check the spatial calibration of each objective. Fluorescent microspheres with mixtures of fluorophores (FluoSpheres; Molecular Probes) are useful for checking the  $x,y$  and axial alignment of images acquired at different excitation wavelengths. Misalignment of the images in the  $xy$  plane may indicate that the pinholes are not centered or that the lasers need to be aligned; misalignment in the  $z$  axis may be due to incorrect setting of a collimating lens, misalignment of pinholes, or chromatic aberration in the objective. The optical resolution of the microscope can be measured by capturing images of submicroscopic ( $<0.2$  nm) fluorescent microspheres (Fig. 2C.1.2C,G). The images of the microspheres should be radially symmetrical in the  $xy$  plane and elliptical in the  $z$ -axis (Fig. 2C.1.2C). Horizontal and axial resolutions are defined by the full width at half maximal intensity (FWHM) of intensity profiles along the horizontal and vertical axes of the beads (Fig. 2C.1.2D,H).

## Anticipated Results

Confocal microscopy provides sharp images of fluorescent structures in thick specimens (Fig. 2C.1.1, Fig. 2C.1.2, Fig. 2C.1.3C, D). The maximum depth at which adequate images can be obtained depends on the objective and the optical properties of the specimen. With a high-NA immersion objective, it may be possible to capture images at depths of  $>100$   $\mu\text{m}$  in a specimen that is transparent and not heavily stained (Centonze and Pawley, 1995). However, if the specimen scatters light, both the illumination intensity and the proportion

of the emitted fluorescence that is captured by the objective decline with increasing focal depth. Mismatch of the refractive indexes of the immersion medium and specimen will further reduce the depth at which adequate signal can be obtained. A low-NA objective can capture images at greater depths but provides much poorer axial resolution.

A three-dimensional reconstruction of the specimen can be generated from a series of optical sections at appropriately spaced intervals along the optical axis. The reconstruction can be viewed from any angle, but the view along the optical axis of the objective will appear sharper than off-axial views, because the lateral resolution of the objective is better than the axial resolution (Fig. 2C.1.2). The axial distortion can be corrected by computational deconvolution (Wouterlood, 2005).

Confocal imaging in living specimens is feasible although care must be taken to avoid phototoxicity and photodamage. Robust fluorophores such as the fluorescent proteins EGFP and EYFP can be imaged hundreds of times with minimal photobleaching and no apparent phototoxicity, provided that the illumination is kept at a low level. Synthetic fluorophores, such as organelle-specific dyes (Molecular Probes), generally are more photosensitive, although in some applications the rate of bleaching can be reduced by the addition of Oxyrase. The maximum rate at which images can be collected will depend on the scan speed, resolution, and area. Typical scan times for a  $512 \times 512$  image are 1 to 4 sec/frame.

A common application of confocal microscopy is to determine the relative distributions and extent of colocalization of the molecules tagged with different fluorophores (Brelje et al., 2002). As many as four different fluorophores can be discriminated on a confocal microscope with laser excitation at 350/405, 488, 546/568, and 633/647 nm, and standard photodetectors, provided that the excitation spectra of the fluorophores are well separated and matched to the laser lines. Confocal microscopes with spectral detectors can discriminate larger combinations of fluorophores on the basis of their emission spectra. Spectral detection and linear unmixing allows discrimination of fluorophores with highly overlapping emission spectra, such as GFP and YFP (Dickinson, et al., 2001).

Confocal microscopy also is well suited for visualizing variants of the green fluorescent protein. CFP and YFP can be visualized with minimal cross-talk between channels on a con-

focal microscope with 405 nm and 514 nm excitation. The overlap of the excitation and emission spectra of CFP and GFP or GFP and DsRed may result in cross-talk between channels in experiments with these combinations of fluorophores. New fluorescent proteins have been developed that potentially could provide more optimal combinations for multi-color imaging (Shaner et al., 2004). Fluorescent proteins have also been incorporated into biochemical reporters for measuring intracellular calcium, kinase activity, and other signaling molecules (Zhang et al., 2002).

Photosensitive fluorescent proteins are available that undergo a change in spectral properties upon photoactivation. Photactivatable GFP (PaGFP; Patterson and Lippincott-Schwartz, 2002) exhibits little fluorescence under 488 nm illumination prior to activation but undergoes a 100-fold increase in fluorescence after photoactivation at 400 to 430 nm. An LSCM with a 405- or 413-nm laser can be used to photoactivate PaGFP within a user-defined region of interest within the specimen and thereby selectively “highlight” GFP fluorescence within that region. The activated GFP retains its fluorescence indefinitely and, importantly, manifests these properties even when fused to another protein. PaGFP fusion proteins provide a useful tool for studying the intracellular dynamics of proteins and organelles (Karbowksi et al., 2004).

LSCMs that incorporate an AOTF to control the illumination wavelength and intensity can be configured to perform various types of photobleach experiments. Measurement of fluorescence recovery after photobleach (FRAP) or fluorescence loss in photobleach (FLIP) can provide information about molecular mobility and binding (Cole et al., 1996; McNally and Smith, 2002; Lippincott-Schwartz et al., 2003). In FRAP, fluorescence in a small region of the specimen is photobleached by scanning with high-intensity illumination, and recovery of fluorescence into the bleached area is then monitored by scanning with low-intensity illumination. The rate of return of fluorescent molecules into the bleached area may be governed by diffusion, binding interactions with other molecules, or a combination of both, and appropriate mathematical models have been developed to analyze these responses (Sprague and McNally, 2005). In FLIP, a region of the specimen is photobleached several times with a delay between the bleach scans and images are collected during this process to monitor the distributions of bleached and nonbleached fluorescent molecules. Observation of FLIP can

show whether there is exchange of fluorescent molecules between two compartments of a cell or whether a fluorescent structure is a single organelle or a network of contiguous but independent organelles (Cole et al., 1996).

The spatial precision by which two fluorophores can be said to colocalize on the basis of light microscopy is limited by the optical resolution ( $\sim 0.2 \mu\text{m}$  in the  $xy$  plane and  $0.6 \mu\text{m}$  in the  $z$ -axis). The phenomenon of fluorescence resonance energy transfer (FRET) can potentially reveal whether two fluorophores are within  $<10 \text{ nm}$  proximity. FRET (Wouters and Bastiaens, 2000) is the nonradiative transfer of energy from a fluorescent donor molecule to an acceptor molecule. Energy transfer occurs only if the molecules are within a distance of less than  $\sim 10 \text{ nm}$ , and only if the emission spectrum of the donor overlaps the excitation spectrum of the acceptor. One application of FRET is to determine whether two populations of molecules undergo binding interactions. One population is labeled with donor fluorophores (e.g., CFP) and the second is labeled with acceptor fluorophores (e.g., YFP). Several techniques for measuring FRET have been devised (Jares-Erijman and Jovin, 2003) and many of these can be carried out with current LSCMs.

Current LSCMs are much superior to their predecessors in sensitivity, speed of image acquisition and versatility. Although they are expensive (\$200,000 to \$600,000) and require costly service contracts to ensure optimal performance, their many benefits justify these costs.

### Acknowledgements

The author wishes to thank Dr. Albert Neuztner (National Institutes of Health, Bethesda, Md.) for providing the cells illustrated in Fig. 2C.1.3 and Dr. James Galbraith (also of the National Institutes of Health) for helpful comments on the manuscript. This research was supported by the Intramural Research Program of the National Institute of Neurological Diseases and Stroke at the National Institutes of Health, Bethesda, Md.

### LITERATURE CITED

Ando, R., Hama, H., Yamamoto-Hino, M., Mizuno, H., and Miyawaki, A. 2002. An optical marker based on the UV-induced green-to-red photo-conversion of a fluorescent protein. *Proc. Natl. Acad. Sci. U.S.A.* 99:12651-12656.

Art, J. 1995. Photon detectors for confocal microscopy. *In Handbook of Biological Confocal Microscopy*, 2nd ed. (J. Pawley, ed.) pp. 183-196. Plenum, New York.

Bacallao, R., Kiai, K., and Jesaitis, L. 1995. Guiding principles of specimen preservation for confocal fluorescence microscopy. *In Handbook of Biological Confocal Microscopy*, 2nd ed. (J. Pawley, ed.) pp. 311-326. Plenum, New York.

Benham, G. 2002. Practical aspects of objective lens selection for confocal and multiphoton digital imaging techniques. *In Cell Biological Applications of Confocal Microscopy*, 2nd ed. (B. Matsumoto, ed.) pp. 247-300. Academic Press, San Diego, Calif.

Boccacci, P. and Bertero, M. 2002. Image-restoration methods: Basics and algorithms. *In Confocal and Two-Photon Microscopy: Foundations, Applications, and Advances* (A. Diaspro, A., ed.), pp. 253-269. John Wiley & Sons, Hoboken, N.J.

Brelje, T.C., Wessendorf, M.W., and Sorenson, R.L. 1993. Multicolor laser scanning confocal immunofluorescence microscopy: Practical applications and limitations. *In Cell Biological Applications of Confocal Microscopy* (B. Matsumoto, ed.) pp. 98-182. Academic Press, San Diego, Calif.

Brelje, T.C., Wessendorf, M.W., and Sorenson, R.L. 2002. Multicolor laser scanning confocal immunofluorescence microscopy: Practical applications and limitations. *In Cell Biological Applications of Confocal Microscopy*, 2nd ed. (B. Matsumoto, ed.), pp. 166-244. Academic Press, San Diego, Calif.

Centonze, V. and Pawley, J. 1995. Tutorial on practical confocal microscopy and use of the confocal test specimen. *In Handbook of Biological Confocal Microscopy*, 2nd ed. (J. Pawley, ed.) pp. 549-570. Plenum, New York.

Cole, N., Smith, C., Sciaky, N., Terasaki, M., Edidin, M., and Lippincott-Schwartz, J. 1996. Diffusional mobility of Golgi proteins in membranes of living cells. *Science* 237:797-801.

Daims, H., Lucker, S., and Wagner, M. 2006. *Daime*, a novel image analysis program for microbial ecology and biofilm research. *Environ. Microbiol.* 8:200-213.

Diaspro, A. (ed.) 2002. *Confocal and Two Photon Microscopy: Foundations, Applications and Advances*. Wiley-Liss, New York.

Dickinson, M.E., Bearman, G., Tille, S., Lansford, R., and Fraser, S.E. 2001. Multi-spectral imaging and linear unmixing add a whole new dimension to laser scanning fluorescence microscopy. *Biotechniques* 31:1274-1278.

Drenkard, E. and Ausubel, F.M. 2002. *Pseudomonas* biofilm formation and antibiotic resistance are linked to phenotypic variation. *Nature* 416:740-743.

Elphick, G.F., Querbes, W., Jordan, J.A. Gee, G.V., Eash, S., Manley, K., Dugan, A., Stanifer, M., Bhatnagar, A., Koreze, W.K., Roth, B.L., and Atwood, J.W. 2004. The Human Polyomavirus, JCV, uses serotonin receptors to infect cells. *Science* 306:1380-1383.

Ferrari, A., Pellegrini, V., Arcangeli, C., Fittipaldi, A., Giacca, M., and Beltram, F. 2003. Caveolae-mediated internalization of extracellular HIV-1

- Tat fusion proteins visualized in real time. *Mol. Ther.* 8:284-294.
- Forest, T., Barnard, S., and Baines, J.D. 2005. Active intranuclear movement of herpes virus capsids. *Nat. Cell Biol.* 7:429-431.
- Giloh, H. and Sedat, J.W. 1982. Fluorescence microscopy: Reduced photobleaching of rhodamine and fluorescein protein conjugates by *n*-propyl gallate. *Science* 217:1252-1255.
- Glushakova, S., Yin, D., Li, T., and Zimmerberg, J. 2005. Membrane transformation during malaria parasite release from human red blood cells. *Curr. Biol.* 15:1645-1650.
- Inoué, S. and Inoué, T. 2002. Direct-View High-Speed Confocal Scanner: The CSU-10. In *Cell Biological Applications of Confocal Microscopy*, 2<sup>nd</sup> ed. (B. Matsumoto, ed.) pp. 88-128. Academic Press, San Diego, Calif.
- Inoué, S. and Spring, K.R. 1997. *Video Microscopy: The Fundamentals*, 2nd ed. Plenum, New York.
- Jares-Erijman, E.A. and Jovin, T.M. 2003. FRET imaging. *Nat. Biotechnol.* 21:1387-1395.
- Johnson, G.D., Davidson, R.S., McNamee, K.C., Russell, G., Goodwin, D., and Holborow, E.J. 1982. Fading of immunofluorescence during microscopy: A study of the phenomenon and its remedy. *J. Immunol. Methods* 55:231-242.
- Kamabadur, R., Koizumi, K., Stivers, C., Nagle, J., Poole, S., and Odenwald, W. 1998. Regulation of *POU* genes by *castor* and *hunchback* establishes layered compartments in the *Drosophila* CNS. *Genes Dev.* 12:246-260.
- Karbowski, M., Arnoult, D., Chen, H., Chan, D.C., Smith, C.L., and Youle, R.J. 2004. Quantitation of mitochondrial dynamics by photolabeling of individual organelles shows that mitochondrial fusion is blocked during the Bax activation phase of apoptosis. *J. Cell Biol.* 164:493-499.
- Keller, E. 1995. Objective lenses for confocal microscopy. In *Handbook of Biological Confocal Microscopy*, 2nd ed. (J. Pawley, ed.) pp. 111-126. Plenum, New York.
- Lippincott-Schwartz, J., Altan-Bonnet, N., and Patterson, G.H. 2003. Photobleaching and photoactivation: Following protein dynamics in living cells. *Nat. Cell Biol.* Suppl:S7-S14.
- Majlof, L. and Forsgren, P. 2002. Confocal microscopy: Important considerations for accurate imaging. In *Cell Biological Applications of Confocal Microscopy* 2nd ed. (B. Matsumoto, ed.) pp. 149-164. Academic Press, San Diego, Calif.
- Matsumoto, B. (ed.) 2002. *Cell Biological Applications of Confocal Microscopy*. 2nd ed. Academic Press, London.
- McNally, J., Karpova, T., Cooper, J., and Conchello, J. 1999. Three-dimensional imaging by deconvolution microscopy. *Methods* 19:373-385.
- McNally, J.G. and Smith, C.L. 2002. Photobleaching by confocal microscopy. In *Confocal and Two Photon Microscopy: Foundations, Applications and Advances* (A. Diaspro, ed.) pp. 525-538. Wiley-Liss, New York.
- Nerbonne, J.M. 1996. Caged compounds: Tools for illuminating neuronal responses and connections. *Curr. Opin. Neurobiol.* 6:379-386.
- Patterson, G.H. and Lippincott-Schwartz, J. 2002. A photoactivatable GFP for selective photolabeling of proteins and cells. *Science* 297:1873-1877.
- Perrin, A.J., Jiang, X., Birmingham, C.L., So, N.S., Burmell, J.H. 2004. Recognition of bacteria in the cytosol of mammalian cells by the ubiquitin system. *Curr. Biol.* 14:806-811.
- Rani, S.A., Pitts, B., and Stewart, P.S. 2005. Rapid diffusion of fluorescent tracers into *Staphylococcus* epidermis biofilms visualized by time lapse microscopy. *Antimicrob. Agents Chemother.* 49:728-732.
- Roux, P., Munter, S., Frischknecht, F., Herbomel, P., and Shorte, P. 2004. Focusing light on infection in four dimensions. *Cell. Microbiol.* 6:333-343.
- Sandison, D.R., Williams, R.M., Wells, K.S., Strickler, J., and Webb, W.W. 1995. Quantitative fluorescence confocal laser scanning microscopy. In *Handbook of Biological Confocal Microscopy*, 2nd ed. (J. Pawley, ed.) pp. 39-54. Plenum, New York.
- Satpute-Krishnan, P., DeGiorgis, J.A., and Bearer, E.L. 2003. Fast anterograde transport of Herpes Simplex Virus: Role for the amyloid precursor protein of Alzheimer's disease. *Aging Cell* 2:305-318.
- Shaner, N.C., Campbell, R.E., Steinbach, P.A., Giepmans, B.N., Palmer, A.E., and Tsien, R.Y. 2004. Improved monomeric red, orange and yellow fluorescent proteins derived from *Discosoma* sp. Red fluorescent protein. *Nat. Biotechnol.* 22:1567-1572.
- Shotton, D.M. 1993. Electronic acquisition of light microscope images. In *Electronic Light Microscopy* (D.M. Shotton, ed.) pp. 1-38. Wiley-Liss, New York.
- Sprague, B.L. and McNally, J.G. 2005. FRAP analysis of binding: Proper and fitting. *Trends Cell Biol.* 15:84-91.
- Terasaki, M. and Dailey, M.E. 1995. Confocal microscopy of living cells. In *Handbook of Biological Confocal Microscopy*, 2nd ed. (J. Pawley, ed.) pp. 327-346. Plenum, New York.
- Tsien, R.Y. and Waggoner, A. 1995. Fluorophores for confocal microscopy. In *Handbook of Biological Confocal Microscopy*, 2nd ed. (J. Pawley, ed.) pp. 267-280. Plenum, New York.
- Viachou, D., Zimmermann, T., Cantera, R., Janse, C.J., Waters, A.P., and Kafatos, F.C. 2004. Real-time, in vivo analysis of malaria ookinete locomotion and mosquito midgut invasion. *Cell Microbiol.* 6:671-685.
- Waterman-Storer, C.M., Sanger, J.W., and Sanger, J.M. 1993. Dynamics of organelles in the mitotic spindles of living cells: Membrane and microtubule interactions. *Cell Motil. Cytoskeleton* 26:19-39.
- Webb, R.H. and Dorey, C.K. 1995. The pixilated image. In *Handbook of Biological Confocal*

Microscopy, 2nd ed. (J. Pawley, ed.) pp. 55-68. Plenum, New York.

Wilson, T. (ed.) 1990. Confocal Microscopy. Academic Press, London.

Wilson, T. 1995. The role of the pinhole in confocal imaging system. *In Handbook of Biological Confocal Microscopy*, 2nd ed. (J. Pawley, ed.) pp. 167-182. Plenum, New York.

Wouterlood, F.G. 2005. 3-D reconstruction of neurons from multichannel confocal laser scanning image series. *In Current Protocols in Neuroscience* (J.N. Crawley, C.R. Gerfen, M.A. Rogawski, D.R. Sibley, P. Skolnick, and S. Wray, eds) pp. 2.8.1-2.2.8.16. John Wiley & Sons, Hoboken, N.J.

Wouters, F.S., and Bastiaens, P.I.H. 2000. Imaging protein-protein interactions by fluorescence resonance energy transfer (FRET) microscopy. *In Current Protocols in Cell Biology* (J.S. Bonifacino, M. Dasso, J.B. Harford, J. Lippincott-Schwartz, and K.M. Yamada, eds.) pp. 17.1.1-17.1.15. John Wiley & Sons, Hoboken, N.J.

Zhang, J., Campbell, R.E, Ting, A., and Tsien, R.Y. 2002. Creating new fluorescent probes for cell biology. *Nature Rev. Mol. Cell Biol.* 3:906-918.

## KEY REFERENCES

Inoué and Spring, 1997. See above.

*Covers the basics of light microscopy, video microscopy, and much more.*

Matsumoto, 2002. See above.

*Good source of practical information about confocal imaging.*

Pawley, J. (ed.) 1995. See above.

*Comprehensive reference book on confocal microscopy.*

Russ, J. 2002. *The Image Processing Handbook*. 4th edition. CRC Press, Boca Raton, Fla.

*Guide to digital image processing.*

## INTERNET RESOURCES

<http://www.microbial-ecology.net/daime>

*Daime Web site, from which the Daime software application can be downloaded. Daime (digital image analysis in microbial ecology) is an open-source software program for 2-D and 3-D image analysis developed by Holger Daims, Sebastian Lückner, and Michael Wagner (Universität Wien, Vienna, Austria). The features of Daime and its application to analysis of biofilms are described in Daims et al. (2006).*

<http://rsb.info.nih.gov/ij>

*ImageJ is a public domain image analysis program developed by W. Rasband (Research Services Branch, National Institute of Mental Health, NIH) for operating systems running Java (including Windows/PC and OSX/Macintosh). ImageJ has many useful tools for analysis of confocal images.*

<http://www.uhnres.utoronto.ca/facilities/wcif/imagej/>

*A manual written by Tony Collins that describes the use of ImageJ to visualize and analyze confocal images.*

<http://www.molecularexpressions.com>

*The Molecular Expressions Web site is a rich source of information about all aspects of light microscopy, including confocal microscopy. It includes sections on the basic principles of confocal imaging, instrumentation, sample preparation, and choices of fluorophores. An interactive tutorial "Choosing fluorophore combinations for confocal microscopy" allows the user to determine the extent of spectral cross-over that will occur when imaging different combinations of fluorophores with specific laser lines and filter sets.*

## Web sites of vendors of confocal microscopes

*These provide product descriptions, manuals, tutorials and literature.*

<http://www.zeiss.com>

*Carl Zeiss, Inc.*

<http://www.leica-microsystems.com/company>

*Leica Microsystems.*

<http://www.nikonusa.com>

*Nikon, Inc.*

<http://www.microscopyu.com>

*For information about light microscopy and confocal microscopy.*

<http://www.olympusconfocal.com/>

*Olympus, Inc.*

<http://www.perkinelmer.com/>

*PerkinElmer, Inc.*

<http://www.solamereotech.com/>

*Solamere Technology.*

## Spectra of fluorophores

<http://fluorescence.nexus-solutions.net/frames6.htm>

*Biorad Microsciences fluorochrome database and charting application.*

<http://home.earthlink.net/~fluorescentdyes/>

*George McNamara Multiprobe Microscopy.*

<http://www.probes.com/>

*Molecular Probes.*

<http://www.molecularexpressions.com>

*Molecular Expressions.*

<http://www.olympusfluoview.com/resources/specimenchambers.html>

*Sources of chambers for maintaining living specimens during observation by microscopy.*

<http://listserv.buffalo.edu/user/sub.html>

*Many topics of interest to confocal microscopists are discussed on the confocal listserv operated by the listserv at the University at Buffalo. To subscribe to the list go to the URL and type "confocal" in the box that asks which list one wishes to join.*

---

Contributed by Carolyn L. Smith  
National Institute of Neurological  
Disorders and Stroke  
Bethesda, Maryland